Position and Velocity Analysis of Free-Ended Two-Link Object for Whole Arm Manipulation

تحليل الموضع والسرعة لهدف حر- الطرفين ذو- وصلتين للمناولة بكامل الذراع

Zakarya Zyada
RIKEN, 2270-130 Anagahora, Shimoshidami, Moriyama-ku, Nagoya 463-0003, Japan
(Faculty of Engineering, Tanta University, Tanta, Egypt)
E-mail: zzyada@nagoya.riken.jp; zzyada@yahoo.com

الخلاصة :
هذا البحث يقدم تحليل الموضع والسرعة لهدف حر- الطرفين ذو- وصلتين جاسئتين لمناولته بذراعين كتبسيط أولى لإمساك ومناولة جسم انسان بواسطة روبوت انسانى. يتم شرح الدحرجة والانزلاق عند نقاط الإتصال الخاصة بالهدف ذو الوصلتين والمقيد بالذراعين الحاملين. يتم تقديم تحليل الموضع والسرعة للهدف المراد تناوله، قيود الموضع والسرعة وكذلك العبارات الجبرية لمسافة وسرعة الإنزلاق. يتم تقديم نتائج المحاكاة لمسافات وسرعات الإنزلاق، ومسافات وسرعات وصلات الهدف وكذلك شكل الهدف عند مدخلات ذات سرعات دحرجة مختلفة.
ما تم تقديمه من تحليل الموضع والسرعة يبرهن على :1- من خلال مناولة هدف ذو وصلتين بواسطة ذراعين، فإن الدحرجة عند نقطة أو كلا نقطتى الاتصال مقترن بالانزلاق عند كلا نقطتى الاتصال. لا يوجد دحرجة بدون انزلاق ولا يوجد انزلاق بدون دحرجة. 2- من الممكن أن نعرف شكل الهدف من نقاط الاتصال، وبالتالى من قياسات زوايا الاتصال باستخدام حساسات اللمس . 3- من الممكن حساب مسافة الانزلاق عند كلا نقطتى الاتصال من قياسات زوايا الاتصال لمرتين متعاقبتين . 4- من الممكن أن نعرف سرعات وصلات الهدف وكذلك سرعات الانزلاق من استنباطات أو قياسات سرعات الدحرجة.

Abstract—this paper presents position and velocity analysis of free-ended two-rigid-links object manipulated by two arms as an initial step simplification of holding and manipulating a human body by a humanoid robot. Rolling as well as sliding at the points of contact of the two-links object constrained by the holding two-arms is explained. Position and velocity analysis of the manipulated object, position and velocity constraints as well as expressions for sliding displacement and sliding velocity are presented. Simulation results for sliding displacement, sliding velocity, object links displacements and velocities as well as object configurations for different input rolling velocities are presented. The presented position and velocity analysis proves that: 1- through manipulating two-links object by two-arms, rolling at one point or both points of contact is associated with sliding at both points of contact. There is no rolling without sliding and there is no sliding without rolling. 2- It is possible to define the configuration of the object from contact points and hence contact angle measurements applying tactile sensors. 3- It is possible to compute the amount of sliding at both contact points from consecutive contact angle measurements. 4- It is possible to define the object links velocity as well as sliding velocity from the contact rolling velocities estimations or measurements.

I. INTRODUCTION

Human interactive robotics has received a considerable attention by different research groups seeking their promising human-friendly assist and cooperation. Among these groups is RIKEN robotics research group who introduced RI-MAN for holding and transferring a patient, [1], [2]. RI-MAN is designed to grasp, hold and transfer a human applying its whole two-arms, Fig. 1. Whole arm manipulation is an approach to manipulation that employs all the available manipulation surfaces of the robot to act upon and sense the environment, [3]. Restraining large size objects, lifting heavy loads or assembling mating parts are examples of suitable tasks that require whole arm manipulation. Whole arm grasps are formed by wrapping the arms (or fingers) around the objects, [4]. Manipulating a human, (the task is a patient), as shown in Fig. 1, lies in the taxonomy of dynamic manipulation in which task dynamics is significant for analysis and planning. Kinematic, static and quasi-static manipulation analysis is important steps for dynamic manipulation. Dynamic manipulation has many benefits such as increasing the repertoire of actions to manipulators, increasing

Accepted September 9, 2009.

the speed of manipulation and saving the complexity and the mass of the robot, [5]. With dynamic manipulation, some of the complexity of the robot system is transferred from the hardware (joints and actuators) to planning and control, [6]. Many research works for different dynamic manipulation tasks can be found in the literature. Motion planning of a 1-DOF dynamic pitching robot throwing a ball in a horizontal plane is presented in [7]. Dynamic manipulation of an object over a plate inspired by the handling of a pizza peel is presented in [8]. Motion planning and controllability for nonprehensile (without a form- or force-closure) manipulation for throwing and catching a disc using two planar manipulators are presented in [9]. Carrying a polygonal shape object applying two mobile robots with nonprehensile manipulators has been presented in [10]. So far the presented work is concerned with one-link object to be manipulated by one or two manipulators. However an application like holding and/or transferring a human, (patient for instance), is an example of multi-link object which is not tackled in research literature, (up to the author's knowledge), in robotics manipulation. To define, apply and assure stable holding and manipulating as well as control, it is important to analyze and understand kinematics and dynamics of the manipulated multi-link object. As an initial step towards analysis of holding and manipulating a human body object, this paper introduces two-dimensional position and velocity analysis of free ended two-link rigid body object hold by two arms, Fig. 3. Kinematic relations as well as kinematic constraints are to be introduced. Through analysis and simulation, it is aimed to answer the following questions:

1- given the points of contact, (and hence the angles of contact) , for a two-link object hold by two-arms, at any instant:
   a) Is it possible to get information about the object configuration?
   b) Is it possible to get information about sliding amounts of the object links over the arms?
   c) How are rolling and sliding displacements associated with each other?

Fig. 1. RIMAN holding a dummy patient, [2]

2- given the rate of change of angles of contact or rolling velocity:
   a) Is it possible to get information about object-links different velocities?
   b) Is it possible to get information about the sliding velocities of links over arms?
   c) How are links sliding velocities associated with rolling velocities?

This paper is organized as follows: rolling and sliding of one link object over one arm in a plane is presented in section II. Position analysis of two-link object constrained by two-arms with rolling and sliding motions, position constraints, sliding displacement expressions and position simulation results are introduced in section III. Velocity analysis of two-link object constrained by two-arms, velocity constraints, sliding velocity expressions and the velocity simulation results for different rolling velocities are introduced in section IV. Conclusion and directions for future work are to be presented in section V.

II. Rolling and Sliding of One Link Object

In this section, rolling and/or sliding of a slem rigid-link object over a rigid-link arm system, Fig. 2 is explained. Contact type is assumed to be hard contact. The coordinate system is introduced first followed by explanation of the different possible rolling and/or sliding motions.

A. Coordinate system

The coordinate system is defined as shown in Fig. 2. A reference coordinate frame 0, $O_0 - x_0 y_0$

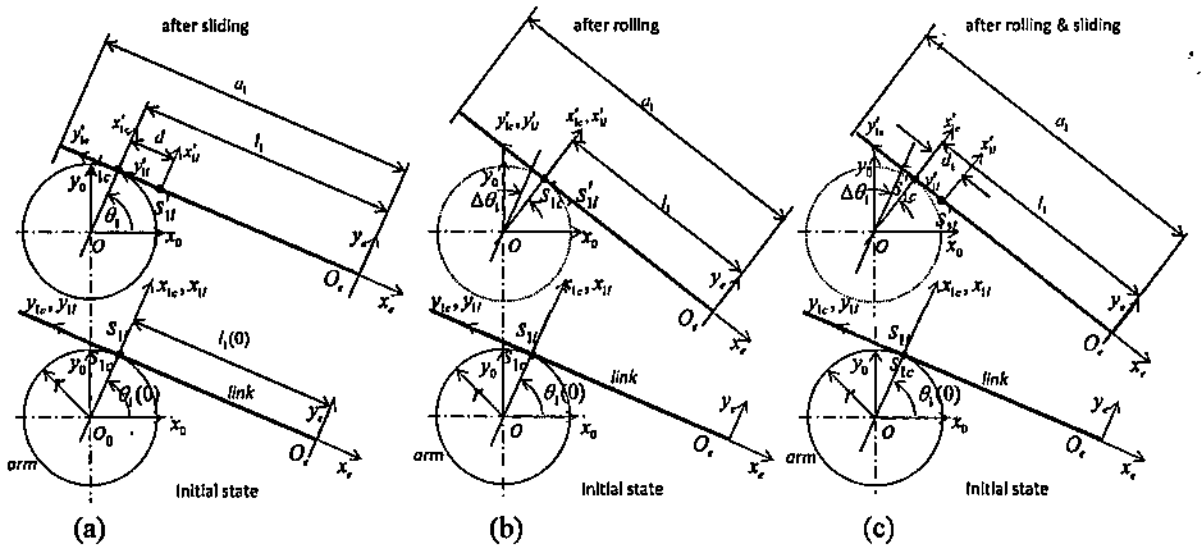

Fig. 2. Graphical representation of rolling and/or sliding motion of a link over an arm, (lower graph: before motion; upper graph: after motion); (a) sliding motion only, (b) rolling motion only, (c) both rolling and sliding motion.

is defined at the center of the circular cross section of the arm; two frames S_{1l} and S_{1c} both initially having the origin at the point of contact between the link and the arm, s_1 are also defined. Frame S_{1l}, $(O_{1l} - x_{1l}y_{1l})$, is fixed to the link while frame S_{1c}, $(O_{1c} - x_{1c}y_{1c})$, is at the point of contact between the link and the arm; x_{1c} is in the dirction of line from O_0 to s_1 which is also normal to the plane including the point of contact as shown in Fig. 2. Frame e, $O_e - x_e y_e$ is attached to the right end of the arm. The angle θ_1, denoted as the angle of contact, is measured from x_0 to x_{1c} and being positive counter clockwise; the length l_1 expresses link segment length from the origin of frame S_{1c} to the origin of frame e. The total length of the object link is a_1; Clearly l_1 is a variable while a_1 is a constant.

The rolling and/or sliding motion between the link object and the arm can be clarified in terms of the relative position of the two reference frames S_{1l} and S_{1c} before and after the motion. After a motion of rolling and/or sliding, frames S_{1l} and S_{1c} are denoted by $S_{1l}^{'}$ and $S_{1c}^{'}$ respectively. Knowing the initial angle of contact $\theta_1(0)$ and the initial length $l_1(0)$ and defining the motion, (rolling and/or sliding), the change in angle of contact $\Delta\theta_1$ and the change in length Δl_1 can be defined. To explain the motions, three cases are considered: 1) sliding of the link over the arm (without rolling); 2) rolling of the link over the arm (without sliding); and 3) both sliding and rolling of the link over the arm.

B. Sliding (without rolling)

Assuming that the link has the possibility to slide (without rolling) over arm, then the contact point after sliding will remain at its location before sliding, ($S_{1c}^{'}$ will be identical to S_{1c}). Hence the angle of contact after sliding, θ_1, will be equal to the initial angle of contact, $\theta_1(0)$, then

$$\Delta\theta_1 = \theta_1 - \theta_1(0) = 0 \qquad (1)$$

Moreover the frame on the link side S_{1l} as well as the whole link will move according to the amount of sliding displacement, d_1. S_{1l} will become in a new position $S_{1l}^{'}$. The length l_1 after sliding, will depend on its initial length, $l_1(0)$, and amount of sliding d_1.

$$\Delta l_1 = l_1 - l_1(0) = d_1 \qquad (2)$$

C. Rolling (without sliding)

Assuming that the link has the possibility to roll without sliding, then both S_{1c} and S_{1l} will be identical and move on the circle of radius r, (the peripheral of the arm), with the amount of rolling distance, $r\Delta\theta_1$, to another position denoted by $S_{1c}^{'}$ and $S_{1l}^{'}$. The change in the angle of contact $\Delta\theta_1$ is a

function of the angle of contact after rolling, θ_1, and the initial angle of contact, $\theta_1(0)$,

$$\Delta\theta_1 = \theta_1 - \theta_1(0) \quad (3)$$

The change in length because of rolling can be defined as:

$$\Delta l_1 = l_1 - l_1(0) = -r\Delta\theta_1 \quad (4)$$

D. Sliding and rolling

Assuming that the link has the possibility to slide and to roll, then both S_{1c} and S_{1l} will move to different new positions according to rolling angle and sliding displacement. S_{1c} will become S'_{1c} according to amount of roll, $r\Delta\theta_1$, while S_{1l} become S'_{1l} according to the amount of sliding, d_1. The new length l_1 will depend on $r\Delta\theta_1$ as well as d_1 and the initial length $l_1(0)$. Expressions for change in the angle of contact and the change in length will be the summation of both the sliding case and the rolling case;

$$\Delta\theta_1 = \theta_1 - \theta_1(0) \quad (5)$$

The change in length because of both sliding and rolling can be defined as:

$$\Delta l_1 = l_1 - l_1(0) = d_1 - r\Delta\theta_1 \quad (6)$$

III. Position Analysis of Constrained Two-Link Object

Understanding the kinematics and dynamics of the human body as an object manipulated by the whole arms of a humanoid robot is important for stable manipulation and control. As an initial step simplification of this difficult problem, the author considers a two-dimensional system of two slender-rigid-link object constrained by two-arms as shown in Fig. 3. In this section position analysis is presented. Sliding and/or rolling motion of two-rigid-link object constrained by two arms is to be presented.

The object is a two free-ended rigid-links, (link 1 and link 2), with total lengths a_1 and a_2 connected with a passive revolute joint. The two-link object is constrained by two arms, (right and left arms). Link 1 has a point contact with the cylindrical right-arm at s_1 while link 2 has a point contact with the cylindrical left-arm at s_2. For the purpose of analysis, the base coordinate frame, (frame b), $o_b - x_b y_b$, the right arm coordinate frame, (frame r), $o_r - x_r y_r$, left-arm coordinate frame, (frame l), $o_l - x_l y_l$, contact points coordinate frames, (frame s_1), $o_{s_1} - x_{s_1} y_{s_1}$ and (frame s_2), $o_{s_2} - x_{s_2} y_{s_2}$', (frame 3), $o_3 - x_3 y_3$ are defined as shown in Fig. 3. The angles of contact, θ_1 is the angle from the x-axis of frame b to the x-axis of frame s_1 while the angle of contact θ_2 is the angle from the x-axis of frame b to the x-axis of frame s_2, Fig. 3, both being positive in a counter clockwise sense. l_1 and l_2 define link segment lengths from origins of frames s_1 and s_2 at the points of contact to the passive joint, origin of frame 3, respectively. It is aimed to get for a two-link manipulated object, constrained as shown in Fig. 3, the constraining relation between l_1, l_2 and θ_1, θ_2.

A. Position of passive joint 3

The position of the passive joint, frame 3, through the right-arm branch, can be described as:

$$p_3^b = p_r^b + r_{r,s_1}^b + R_{s_1}^b r_{s_1,3}^{s_1} \quad (7)$$

where p_r^b is the position vector from the origin of frame b to the origin of frame r expressed in frame b; r_{r,s_1}^b is the position vector from origin of frame r to origin of frame s_1 expressed in frame b; $r_{s_1,3}^{s_1}$ is the position vector from origin of frame s_1 to the origin of frame 3 expressed in frame s_1; and $R_{s_1}^b$ is the rotation matrix from frame s_1 to frame b.

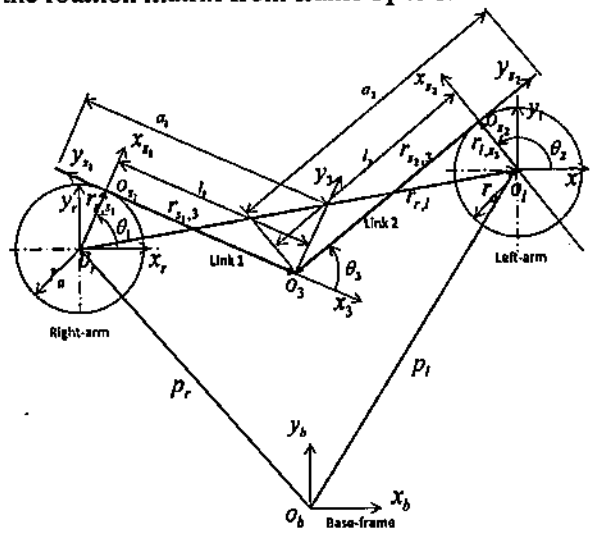

Fig. 3. Coordinate systems of free-ended two-link object by constrained by two-arms

B. Constrained sliding and rolling:

In a similar way, the position of the passive joint, frame 3, through the left-arm branch, can be

described as:

$$p_3^b = p_l^b + r_{l,s_2}^b + R_{s_2}^b r_{s_2,3}^{s_2} \quad (8)$$

where p_l^b is the position vector from the origin of frame b to the origin of frame l expressed in frame b; r_{l,s_2}^b is the position vector from origin of frame l to the origin of frame s_2 expressed in frame b; $r_{s_2,3}^{s_2}$ is the position vector from the origin of frame s_2 to the origin of frame 3 expressed in frame s_2; $R_{s_2}^b$ is the rotation matrix from frame s_2 to frame b. The relative position of the two arms can be expressed as:

$$p_l^b = p_r^b + R_r^b r_{r,l}^r \quad (9)$$

where $r_{r,l}^r$ is the position vector from the origin of frame r to the origin of frame l expressed in frame r; and R_r^b is the rotation matrix from frame r to frame b. Substituting (9) into (8) and equalizing (8) and (7), then

$$r_{r,s_1}^b + R_{s_1}^b r_{s_1,3}^{s_1} = R_r^b r_{r,l}^r + r_{l,s_2}^b + R_{s_2}^b r_{s_2,3}^{s_2} \quad (10)$$

from which, the following constraint equation can be derived,

$$\begin{bmatrix} s\theta_1 & s\theta_2 \\ -c\theta_1 & -c\theta_2 \end{bmatrix} \begin{bmatrix} l_1 \\ l_2 \end{bmatrix} + \begin{bmatrix} x_{r,l} - r_a(c\theta_1 - c\theta_2) \\ y_{r,l} - r_a(s\theta_1 - s\theta_2) \end{bmatrix} = \begin{bmatrix} 0 \\ 0 \end{bmatrix}; \quad (11)$$

where $s\theta_i = \sin(\theta_i)$; $c\theta_i = \cos(\theta_i)$; $x_{r,l}$ and $y_{r,l}$ are the components of position vector $r_{r,l}^r$ in x and y directions respectively; r_a is the radius of both right-arm and left-arm cross section.

C. *Configuration determination from tactile sensors measurements*

Determination of the configuration of the manipulated object is important in dynamic manipulation planning and control. Human do that applying his vision as well as his skin force/position sensors. According to the constraint equation (11), it is possible to define the configuration from tactile sensor measurements. Constraint equation (11) defines the lengths l_1, l_2 in terms of the contact angles θ_1, θ_2 and the relative position of the two-manipulating arms. For given arm size, r_a, relative position, $r_{r,l}^r$, of the two-arms; if it possible to measure (or estimate) the angles of contact θ_1 and θ_2, it is possible to determine the lengths l_1, l_2 which completely define the configuration of the constrained two-links object. Constraint equation (11) clarifies that if roll happens, the configuration will change. Also, in another way, if the configuration of the object is changed, the angles of contact will be changed. Measurements of the angles of contact can be obtained through the tactile sensors proposed by another research team in our institute for the humanoid robot RI-MAN, [11].

TABLE I
SIMULATION PARAMETERS

Parameter	Symbol	Value
Link 1 total length	a_1	0.425 [m]
Link 2 total length	a_2	0.55 [m]
Initial angles of contact		
Relative position of arms:	$\theta_1(0), \theta_2(0)$	70, 110 deg.
- In x-direction	$x_{r,l}$	0.60 [m]
- In y-direction	$y_{r,l}$	0.05 [m]
Arms radii	r_a	0.1 [m]
Sampling time	Δt	0.01 [s]

D. *Rolling-sliding relation*

It is important to define the sliding-rolling relation for future study of planning and control for the current problem of dynamic manipulation. As shown in section II, (equation 6), sliding, d_i, is a function of the change in angle of contact, $\Delta\theta_i$ and the change in length Δl_i for any two system states. The amount of sliding, d_i (referred to the frame s_i), can be expressed as:

$$\begin{matrix} \{d_i = \Delta l_i + r\Delta\theta_i;\ i = 1\} \\ \{d_i = \Delta l_i - r\Delta\theta_i;\ i = 2\} \end{matrix} \quad (12)$$

Given the angles of contact $\theta_i, (i = 1,2)$, (and hence the lengths $l_i, (i = 1,2)$, from equation 11), for any two different instants, the change in length Δl_i, and the change in angle of contact $\Delta\theta_i$ can be obtained, from which the amount of sliding $d_i, (i = 1,2)$, can be estimated at both points of contact. Equation (12) assures that for manipulating two-links by two-arms both rolling and sliding are associated with each other. If roll happened over one or the two arms, sliding at the contact points exist. If sliding at the contact points happened, roll also exists at one or two of contact points. So, if the amount of roll is defined, (as it can be estimated through tactile sensor measurements), the sliding can be defined by (12).

E. Position Simulation Results

A program is implemented in MATLAB to simulate the governing equations of the system presented in this section. Three cases are considered: 1) rolling of link 1 around right arm only, (point of contact s_1 and so the angle of contact θ_1 are changing); the rate of change of the angles of contact considered for simulation are $\dot{\theta}_1 = -30$ deg/s and $\dot{\theta}_2 = 0$ deg/s; 2) rolling of link 2 around left arm only, (point of contact s_2 and so the angle of contact θ_2 are changing); the rate of change of the angles of contact considered for simulation are $\dot{\theta}_1 = 0$ deg/s and $\dot{\theta}_2 = 40$ deg/s; 3) rolling of link 1 around right-arm and rolling of link 2 around left-arm, (points of contact s_1 and s_2 and angles of contact θ_1 and θ_2 are all changing; the rate of change of the angles of contact considered for simulation are $\dot{\theta}_1 = -30$ deg/s and $\dot{\theta}_2 = 40$ deg/s; Simulation parameters are shown in Table I. Simulation results of case 1, case 2 and case 3 are shown in Figs. 4, 5 and 6 respectively.

Shown in Figures 4a, 5a and 6a, the amount of roll, length and sliding displacements of link 1 around right-arm, for the three different cases, (different rates of change of angles of contact). Also shown in Figures 4b, 5b and 6b, the amount of roll, length and sliding displacements of link 2 around left-arm, for the three different cases, (different rates of change of angles of contact as above). These figures assure the association of sliding to roll. Even roll may happen around one arm, the associated sliding exist at both points of contact. The roll is associated with sliding and sliding is associated with rolling.

Shown in Figures 4c, 5c and 6c the position of the passive joint between the two-link object. The positions of passive joint in addition to the contact points completely define the two-link object in the plane. Shown also in Figures 4d, 5d and 6d the configuration changes for the three cases of different contact angles. These figures show that if the angles of contact are measured or estimated by a tactile sensor, the configuration of the object, (which is important for future study of stable dynamic manipulation of two-link object by two-whole-arms), is completely defined.

IV. Velocity Analysis of Constrained Two-Link Object

In this section, the analysis of two-link object constrained by two-arms is extended to include object links' velocities. Velocity of the passive joint is expressed, the velocity constraint equation, the sliding velocity expressions and the simulation results are introduced.

A. Velocity of passive joint 3

Differentiating the position equation (7), the velocity of the passive joint can be obtained,

$$\dot{p}_3^b = \dot{p}_r^b + \dot{r}_{r,s_1}^b + \dot{R}_{s_1}^b r_{s_1,3}^{s_1} + R_{s_1}^b \dot{r}_{s_1,3}^{s_1} \quad (13)$$

where $\dot{r}_{r,s_1}^b = r_a \dot{\theta}_1 [-s\theta_1 \quad c\theta_1 \quad 0]^T$;

$\dot{R}_{s_1}^b(\theta_1) = \begin{bmatrix} -s\theta_1 & -c\theta_1 & 0 \\ c\theta_1 & -s\theta_1 & 0 \\ 0 & 0 & 0 \end{bmatrix} \dot{\theta}_1$; $r_{s_1,3}^{s_1} = [0 \quad l_1 \quad 0]^T$;

$\dot{r}_{s_1,3}^{s_1} = [0 \quad \dot{l}_1 \quad 0]^T$; and $R_{s_1}^b(\theta_1) = \begin{bmatrix} c\theta_1 & -s\theta_1 & 0 \\ s\theta_1 & c\theta_1 & 0 \\ 0 & 0 & 1 \end{bmatrix}$,

$$\begin{bmatrix} \dot{p}_{3x}^b \\ \dot{p}_{3y}^b \end{bmatrix} = \begin{bmatrix} \dot{p}_{rx}^b \\ \dot{p}_{ry}^b \end{bmatrix} + \begin{bmatrix} -r_a s\theta_1 - l_1 c\theta_1 & -s\theta_1 \\ r_a c\theta_1 - l_1 s\theta_1 & c\theta_1 \end{bmatrix} \begin{bmatrix} \dot{\theta}_1 \\ \dot{l}_1 \end{bmatrix} \quad (14)$$

Equation (14) expresses the velocity of the passive joint 3, $\dot{p}_3^b$, as a function of the angle of contact, θ_1, rolling velocity, $\dot{\theta}_1$, the length from the point of contact to the passive joint, l_1, and its rate of change, (the links velocity), $\dot{l}_1$, as well as the velocity of the right arm, frame r, expressed in base frame b, $\dot{p}_r^b$.

B. Velocity constraint equation

Now we would like to get the constraint equation for velocity. In a similar way to above, differentiation is executed for the position of the passive joint, (through the left-arm contact point), of equation (8) from which it is possible to obtain the following velocity equation:

$$\begin{bmatrix} \dot{p}_{3x}^b \\ \dot{p}_{3y}^b \end{bmatrix} = \begin{bmatrix} \dot{p}_{lx}^b \\ \dot{p}_{ly}^b \end{bmatrix} + \begin{bmatrix} -r_a s\theta_2 + l_2 c\theta_2 & s\theta_2 \\ r_a c\theta_2 + l_2 s\theta_2 & -c\theta_2 \end{bmatrix} \begin{bmatrix} \dot{\theta}_2 \\ \dot{l}_2 \end{bmatrix} \quad (15)$$

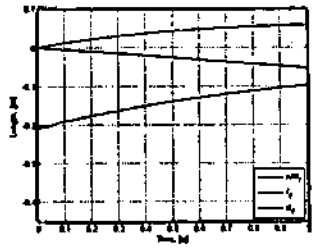

a) roll, length and sliding displacements of link 1around right-arm

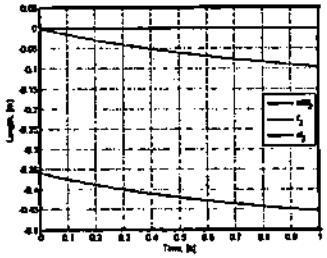

b) roll, length and sliding displacements of link 2 around left-arm

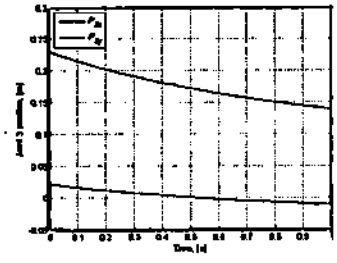

c) position of joint 3

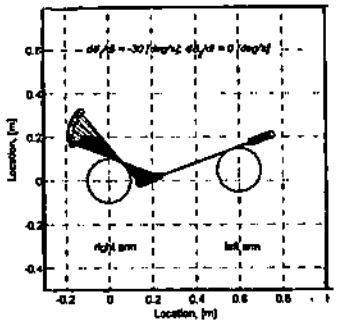

d) configuration changes.

Fig. 4. Simulation results of free-ended two-link object constrained by two-arms for rolling around right-arm only, at s_1, a) roll, length and sliding displacements of link 1around right-arm, b) roll, length and sliding displacements of link 2 around left-arm, c) position of joint 3, d) configuration changes.

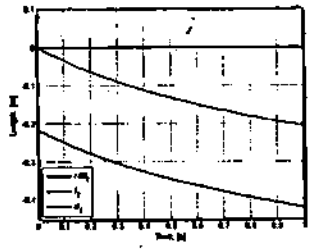

a) roll, length and sliding displacements of link 1around right-arm

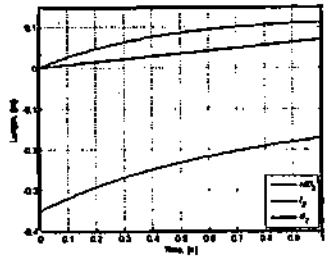

b) roll, length and sliding displacements of link 2 around left-arm

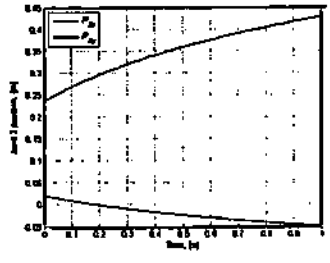

c) position of joint 3

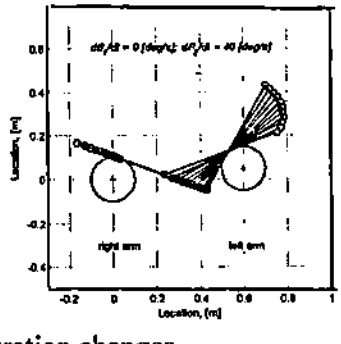

d) configuration changes.

Fig. 5. Simulation results of free-ended two-link object constrained by two-arms for rolling around left-arm only, at s_2, a) roll, length and sliding displacements of link 1around right-arm, b) roll, length and sliding displacements of link 2 around left-arm, c) position of joint 3, d) configuration changes.

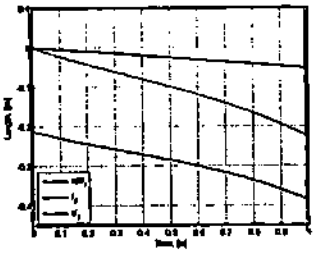

a) roll, length and sliding displacements of link 1around right-arm

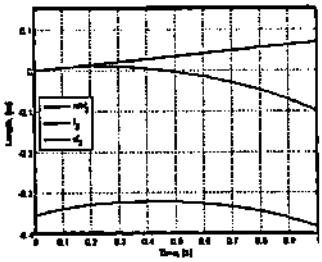

b) roll, length and sliding displacements of link 2 around left-arm

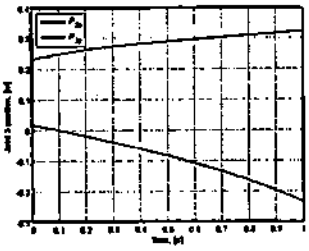

c) position of joint 3

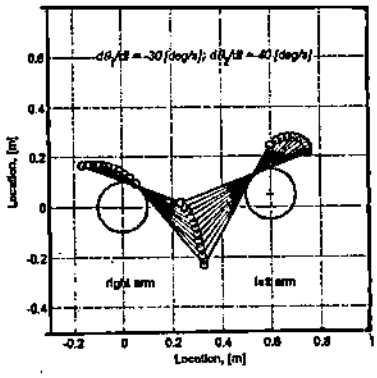

d) configuration changes.

Fig. 6. Simulation results of free-ended two-link object constrained by two-arms for rolling around the respective arms at both s_1 and s_2, a) roll, length and sliding displacements of link 1around right-arm, b) roll, length and sliding displacements of link 2 around left-arm, c) position of joint 3, d) configuration changes.

Differentiating the relative position of the two arms, equation (9), the following rate equation is obtained:

$\dot{p}_l^b = \dot{p}_r^b + \dot{R}_r^b r_{r,l}^r + R_r^b \dot{r}_{r,l}^r$, (assuming $R_r^b = I_3$), then

$$\begin{bmatrix} \dot{p}_{lx}^b \\ \dot{p}_{ly}^b \end{bmatrix} = \begin{bmatrix} \dot{p}_{rx}^b \\ \dot{p}_{ry}^b \end{bmatrix} + \begin{bmatrix} \dot{x}_{r,l} \\ \dot{y}_{r,l} \end{bmatrix} \tag{16}$$

Substituting (16) into (15) and equalizing the right hand side of the result to that of (14), then

$$\begin{bmatrix} s\theta_1 & s\theta_2 \\ -c\theta_1 & -c\theta_2 \end{bmatrix} \begin{bmatrix} \dot{l}_1 \\ \dot{l}_2 \end{bmatrix} + \begin{bmatrix} r_a s\theta_1 + l_1 c\theta_1 & -r_a s\theta_2 + l_2 c\theta_2 \\ -r_a c\theta_1 + l_1 s\theta_1 & r_a c\theta_2 + l_2 s\theta_2 \end{bmatrix} \begin{bmatrix} \dot{\theta}_1 \\ \dot{\theta}_2 \end{bmatrix} + \begin{bmatrix} \dot{x}_{r,l} \\ \dot{y}_{r,l} \end{bmatrix} = \begin{bmatrix} 0 \\ 0 \end{bmatrix} \tag{17}$$

Equation (17) expresses the constraint equation for velocity; for given velocities of rolling, $\dot{\theta}_1$ and $\dot{\theta}_2$, the links velocity, $\dot{l}_1$ and $\dot{l}_2$ are constrained by equation (17) because of the kinematic structure. $\dot{x}_{r,l}$ and $\dot{y}_{r,l}$ are the components of the relative velocity of the left arm with respect to the right arm in x and y directions. The same result can be obtained by differentiating the position constraint equation (11).

C. Sliding velocity estimation

Differentiating equation (12), sliding velocity $\dot{d}_i$ can be obtained as a function of velocity of i^{th} link, $\dot{l}_i$ and velocity of i^{th} rolling velocity, $\dot{\theta}_i$ as follows:

$$\begin{Bmatrix} \dot{d}_i = \dot{l}_i + r\dot{\theta}_i;\ i = 1 \\ \dot{d}_i = \dot{l}_i - r\dot{\theta}_i;\ i = 2 \end{Bmatrix} \tag{18}$$

Estimating the velocities of rolling $\dot{\theta}_1, \dot{\theta}_2$, the velocities of links, $\dot{l}_1, \dot{l}_2$, and sliding velocities $\dot{d}_1, \dot{d}_2$, can be estimated.

D. Velocity Simulation Results

The above equations (17) and (18), (in addition to the position and position constraint equations of section III), are simulated through an implemented MATLAB program. The independent input variables are the contact angle velocities, ($\dot{\theta}_1$ and $\dot{\theta}_2$), and positions, (θ_1 and θ_2). The rolling velocities are assumed as a linear function of time

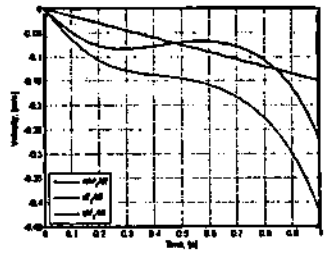

a) roll linear velocity, link velocity and sliding velocity of link 1 over right-arm

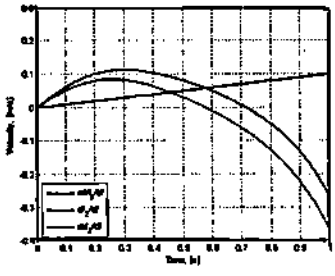

b) roll linear velocity, link velocity and sliding velocity of link 2 over left-arm

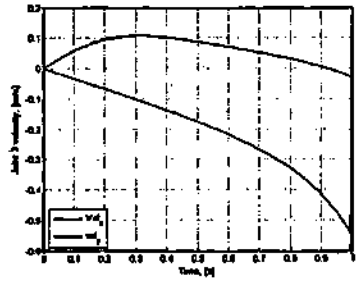

c) Velocity of the passive joint 3

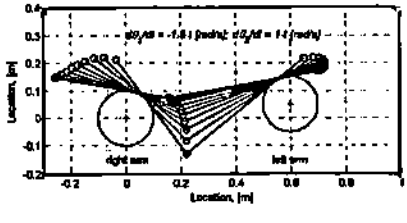

d) Configurations changes

Fig. 7. Simulation results of free-ended two-link object constrained by two-arms for rolling around the respective arms at both s_1 and s_2, a) roll, length and sliding displacements of link 1around right-arm, b) roll, length and sliding displacements of link 2 around left-arm, c) position of joint 3, d) configuration changes.

with different coefficients; $\dot{\theta}_1 = -1.5\,t$ [rad/s]; $\dot{\theta}_2 = t$ [rad/sec]; the angles θ_1 and θ_2 are obtained through integration $\theta_i(t) = \theta_1(t - \Delta t) + \dot{\theta}_i \Delta t$, $i = 1,2$. Δt is the sampling time, assumed to be 0.01 *s*. In real time implementation, the angles of contact can be obtained from tactile sensor measurements and the rates of change can be estimated. The parameters for simulation are as in Table I. the relative velocity of the arms is assumed zero. The simulation results are shown in Fig. 7. The links' velocities and sliding velocities as well as the linear rolling velocity of link 1 over right-arm and the linear rolling velocity of link2 over left-arm are shown in Figures 7a and 7b respectively. These results assure that if it is possible to estimate the velocity of rolling, it is possible to estimate the object links' velocities as well as the sliding velocities. Shown in Figures 7c and 7d, the position of the passive joint 3 and some configurations of the object respectively. Figures show that not only object configuration is detectable but also the object links' velocities.

V. Conclusion

Position and velocity analysis of free-ended two-link object hold by two arms is presented. The main conclusions derived from the presented research work can be summarized as: 1- for dynamic manipulation of two-link object by two arms, rolling of a link about an arm is associated with sliding of the link over the arm at the point of contact. There is no rolling without sliding and there is no sliding without rolling; 2- through the measurements of angles of contact applying a tactile sensor, the configuration of the manipulated two-link object can be determined; 3- through estimating the rolling velocities, links' velocities and the sliding velocities at both points of contact can be estimated. Object configuration determination, sliding displacements and sliding velocities, would facilitate planning and control for dynamic manipulation of the current task.

Future Work

For dynamic analysis and control, it important to analyze forces including gravity forces and friction forces at the points of contact. It is also important

to define stable manipulation and to control object sliding. So, force analysis as well as sliding control for stable manipulation will be of future interest.

ACKNOWLEDGMENT

This work was supported in part by the RIKEN-TRI Collaboration Center for Human-Interactive Robot Research, Nagoya, Japan. The author would like to deeply thank Prof. Yoshikazu Hayakawa, leader of robot research team, RIKEN, Nagoya facility, and Prof. Shigeyuki Hosoe, the manager of the RIKEN-TRI collaboration center for Human Interactive Robotics, Nagoya, for their fruitful discussion during group research meetings and their kind support for hosting the author as 'a foreign postdoctoral researcher' at RIKEN, Nagoya, Japan.

REFERENCES

[1] T. Odashima, M. Onishi, K. Tahara, T. Mukai, S. Hirano, Z. Luo and S. Hosoe, "Development and Evaluation of a Human-interactive Robot Platform "RI-MAN," *Journal of Robotics Society of Japan*, vol. 25, No. 4, pp. 554–565, 2007.

[2] M. Onishi, Z. Luo, T. Odashima, S. Hirano, K. Tahara and T. Mukai, "Generation of Human Care Behaviors by Human-Interactive Robot RI-MAN," in *2007 IEEE International Conference on Robotics and Automation*, pp. 3128–3129.

[3] K. Salisbury, W. Townsend, B. Ebrman and D. DiPietro, "Preliminary Design of a Whole-Arm Manipulation System (WAMS)," in *1988 IEEE International Conference on Robotics and Automation*, pp. 254–260.

[4] P. Song, M. Yashima and V. Kumar, "Dynamics and Control of Whole Arm Grasps," in *2001 IEEE International Conference on Robotics and Automation*, pp. 2229–2234.

[5] M. Mason and K. Lynch, "Dynamic Manipulation," *Proc. Of the 1993 IEEE/RSJ International Conference on Intelligent Robots and Systems*, pp. 152–159.

[6] K. Lynch and M. Mason, "Dynamic Underactuated Nonprehensile Manipulation," *Proceedings of the 2006 IEEE International Conference on Intelligent Robots and Systems*, pp. 889-896.

[7] W. Mori, J. Ueda and T. Ogasawara, "1-DOF Dynamic Pitching Robot that Independently Controls Velocity, Angular velocity, and Direction of a Ball: Contact Models and Motion Planning," in *2009 IEEE International Conference on Robotics and Automation*, pp. 1655–1661.

[8] M. Higashimori, K. Utsumi, Y. Omoto and M. Kaneko, "Dynamic Manipulation Inspired by the Handling of a Pizza Peel," *IEEE Transactions on Robotics*, Vol. 25, No.4, pp. 829-838, 2009.

[9] B. Beigzadeh, M. Ahmadabadi and A. Meghdari, "Two Dimensional Dynamic Manipulation of a Disc Using Two Manipulators," *Proceedings of the 2006 IEEE International Conference on Mechatronics and Automation*, pp. 1191-1196.

[10]A. Gupta and W. Huang, "A Carrying Task for Nonprehensile Mobile Manipulators," *Proceedings of the 2003 IEEE/RSJ International Conference on Intelligent Robots and Systems*, pp. 2896-2901.

[11]T. Mukai, M. Onishi, T. Odashima, S. Hirano, and Z. Luo, "Development of the Tactile Sensor System of a Human-Interactive Robot "RI-MAN"," *IEEE Transactions on Robotics*, Vol. 24, No.2, pp. 505-512, 2008.